Images of cleaved GaAs(110) surfaces observed with a reflection optical second harmonic microscope

H. Sano[a] and T. Shimizu
School of Materials Science, Japan Advanced Institute of Science and Technology, Tatsunokuchi, Ishikawa 923-1292, Japan

G. Mizutani
School of Materials Science, Japan Advanced Institute of Science and Technology, Tatsunokuchi, Ishikawa 923-1292 and "Fields and Reactions," PRESTO, Japan Science and Technology Corporation, 1-1-1 Yanagi-machi, Okayama 700-0904, Japan

S. Ushioda
School of Materials Science, Japan Advanced Institute of Science and Technology, Tatsunokuchi, Ishikawa 923-1292, Japan

(Received 12 July 1999; accepted for publication 11 November 1999)

We have developed a reflection optical second harmonic (SH) microscope as a new surface probe. Using the combination of the developed SH microscope, a near infrared microscope, a confocal laser microscope, a Raman microprobe spectrometer, and an electron probe microanalyzer for x-ray fluorescence, we have observed microstructures on cleaved GaAs(110) surfaces. We have demonstrated that slab structures on these surfaces are unambiguously identified by the analysis using a combination of these microscopes. We have found that the reflection SH microscope is especially sensitive to the slab structures. The enhancement of second harmonic generation by the slab structure could be well accounted for by an electromagnetic calculation of the SH intensity. © *2000 American Institute of Physics.* [S0021-8979(00)09004-6]

I. INTRODUCTION

The spatial variation of physical properties is essentially important in surface and interface phenomena. For example, the microscopic distribution of surface and interface electronic states in MOS structures in LSIs determines the performance of the devices. In the oscillatory catalytic CO oxidation on a Pt(110) surface, distribution of adsorbates shows a spiral pattern and its pattern changes as the oxidation reaction proceeds.[1] In order to clarify the mechanism of these processes, we need a microscope capable of observing electronic states of interfaces buried in devices or surfaces in gaseous environments.

Optical second harmonic generation (SHG) has useful features as a surface probe: SH intensity is highly sensitive to the symmetry at surfaces,[2] and surface electronic states can be obtained by SH spectroscopy.[3,4] We can observe SHG from buried interfaces or surfaces in gaseous environments, so far as the fundamental light beam can reach them. Thus microscopy utilizing this optical process will be a powerful tool in investigating the surface and interface phenomena. However, only a few studies on two-dimensional (2D) mapping of SH signals have so far been reported.[5–8] Thus the development of SH microscopy is one of the urgent needs in surface science.

Transmission SH microscopes were developed by several authors.[7,8] Fiebig *et al.*[7] observed SH intensity images of domain structure of antiferromagnetic Cr_2O_3. In their SH intensity images, domains with opposite orientations of the spin order parameter differed in brightness. Kurimura *et al.*[8] have successfully visualized ferroelectric 180° domains in $LiNbO_3$ and $LiTaO_3$ by using the transmission SH microscope. These references show that the transmission SH microscopes are useful in studying domain structure of certain bulk properties, but they are not suited to surface analysis. Reflection SH microscopes are more suited to surface analysis and have been developed by several authors.[5,6,9] Tanaka *et al.* and Ding *et al.* developed a scanning reflection SH microscope and observed the images of multilayered metal film patterns[5] and organic molecular thin films.[6] Because the signal intensity of reflected SHG is weak, these scanning-type microscopes require a long accumulation time. For example, it took almost a full day to obtain one SH intensity image of a metal film pattern in Ref. 5. Suni has done a quick observation of surface diffusion of In on Ge(111) by a scanning reflection SH microscope, but their mapping of the SH intensity is only one dimensional.[9]

In the present work we have developed a reflection SH microscope equipped with a 2D photodetector. This reflection SH microscope achieves higher resolution (~1 μm) than the scanning SH microscope constructed in our previous work (~100 μm).[5] It requires shorter accumulation time (typically 5–15 min) than our previous one.[5] As a first step of the demonstration of this microscope, we have observed SH intensity images of cleaved GaAs(110) surfaces and have shown that the reflection SH microscope is useful in analyzing the microstructures on surfaces with the size of a few

[a]Author to whom correspondence should be addressed; electronic mail: h-sano@jaist.ac.jp

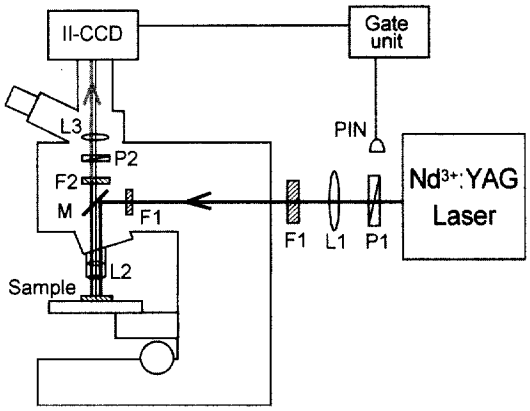

FIG. 1. Reflection SH microscope system. (Li) lens; ($F1$) visible cut filter; ($F2$) bandpass filter; ($P1$) polarizer; ($P2$) analyzer; (M) dichroic mirror; (PIN) pin photodiode. The PIN photo diode picks up the scattering of the excitation laser pulses.

microns. Cleaved GaAs(110) surfaces have various small structures, such as steps, holes, and slabs, produced in cleavage. In order to identify the structures, we also used a near infrared microscope, a confocal laser microscope, a Raman microprobe spectrometer, and an electron probe microanalyzer for x-ray fluorescence. The slab structures on these surfaces are unambiguously identified by the analysis using a combination of these microscopes. We have found that the reflection SH microscope is especially sensitive to the slab structures. The enhancement of SHG by the slab structure could be well accounted for by an electromagnetic calculation of the SH intensity.

II. EXPERIMENT

We have developed a reflection SH microscope system shown in Fig. 1. The incident light for SHG measurements was generated by a mode-locked Ni^{3+}:YAG laser (Continuum PY61-10) with a wavelength of 1064 nm, the pulse duration of 30 ps, and repetition rate of 10 Hz. The excitation beam was incident onto a sample surface after passing through a polarizer, an external lens, a colored glass filter to cut the visible light, the entrance aperture of an optical microscope (Olympus BX60), and its objective lens. The pulse energy of the excitation light beam at the sample surface was 3 μJ/pulse. The reflected SH light from the sample was passed through the objective lens, a bandpass filter with the center wavelength of 532 nm, an analyzer, and finally detected by a charge-coupled device (CCD) camera with a time-gated image intensifier (Hamamatsu PMA-100). The photocathode of the image intensifier in the CCD camera was cooled at about -14 °C. The photon counting function of the CCD system excludes the "Cosmic ray" events during the storage of the SH intensity image. Dark noise of the CCD system with the time-gate width of 1 μs is typically 0.6 cps in a full screen with 640 × 480 channels. The size of the observed area is 0.2–2 mm depending on the magnification of the objective lens from ×50 down to ×5. The spatial resolution is about 1 μm. The developed SH microscope is sensitive enough to detect weak SH signals from a surface, as we have confirmed using a silver film as an example. All SHG measurements were performed in air at room temperature.

First, we note the fidelity of the SH intensity image. A spatial profile of incident light beam may directly affect the quality of the image. In order to check the profile of the incident beam, we often referred to SH intensity images of samples with homogeneous SH response, e.g., cleaved GaAs(110) samples with large mirror-like surfaces. Sometimes a cross-sectional pattern of the incident light beam shows interference fringes. These interference fringes can be easily removed by vibrating the external lens in a plane perpendicular to the optical axis. This operation is effective in improving the fidelity of the image.

In the present study, we have used a configuration of normal incidence and observation, as shown in Fig. 1. This configuration is not appropriate for detecting SH light from the surface of isotropic media, because its surface SH response is generally vanishing for normal incidence. For SH observation from such surfaces, we can modify our SH microscope as follows: the sample shall be tilted by 45° from the optical axis of observation, and collimated incident light shall shine on the sample from outside. In this non-normal configuration, one may fear that the edge of the sample may be out of focus when the center of the sample is properly focused. However, this is not the case when we use the incident light beam with small divergence and see a flat reflecting surface. For example, in the case where we see an image of an area of 1 mmϕ in diameter by using the incident light with beam divergence of 3×10^{-4} rad, the defocusing of the edge of the observed area is calculated to be only about 0.1 μm. This value is smaller than the resolution of our SH microscope. Thus, there is negligible defocusing of the SH intensity image in the non-normal configuration. Actually, we have successfully obtained good SH intensity images with this configuration.[10]

The sample was a GaAs(110) surface cut out by cleavage from a polished wafer of a Si doped n-type GaAs(001) single crystal. The Si concentration was 2.0×10^{18} cm^{-3}, and the wafer thickness was 300 μm. It was mounted on the rotary stage of the SH microscope. Because the crystal structure of GaAs lacks inversion symmetry, it shows a strong bulk SH response. The SH intensity depends on the combinations of incident and output light polarizations and on the sample rotation angle ϕ around its surface normal.[11] We define the sample rotation angle ϕ as the angle between the [001] axis of the GaAs sample and the polarization of the incident light.

In addition to SH microscopy we performed the following observations in order to characterize the microstructures on cleaved GaAs surfaces systematically. (1) With a scanning confocal laser microscope (Olympus OLS1000), topographs of the cleaved surfaces were measured; (2) With a near infrared microscope, images of sample surfaces were taken in order to detect the oscillation of reflectivity as a function of wavelength caused by optical interference in slab structures on the surface. A combination of a halogen lamp, a monochromator (SPEX 270M), a microscope (Olympus BX60), and an infrared viewer (Electrophysics Infrared Elec-

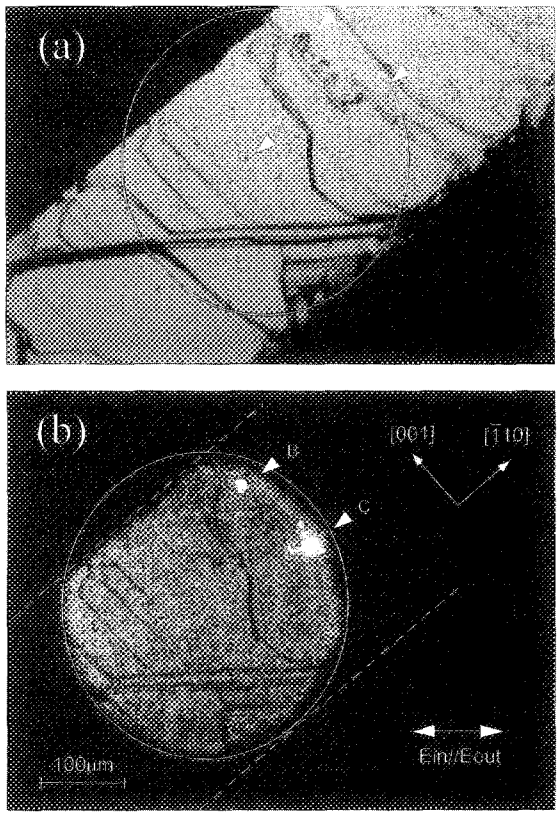

FIG. 2. (a) Microphotograph and (b) a SH intensity image of a cleaved GaAs(110) surface. The sample rotation angle was $\phi=50°$. The incident power and the accumulation time in the SHG measurement were 3 μJ/pulse and 1000 s, respectively.

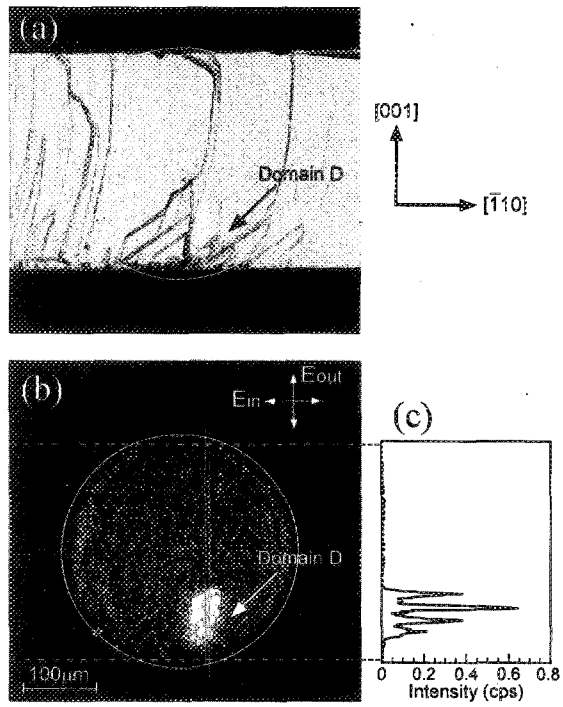

FIG. 3. (a) Microphotograph and (b) SH intensity image of a cleaved GaAs(110) surface near domain *D*. The sample rotation angle is $\phi=90°$. Incident power and accumulation time in the SHG measurement was 3 μJ/pulse and 300 s, respectively. Graph (c) on the right side shows the one-dimensional SH intensity distribution in the region between the two parallel lines in the SH intensity image (b).

tro Viewer 7215) was used to take these images. (3) With an electron probe microanalyzer for x-ray fluorescence (EPMA, JEOL JXA-8900), distribution of atomic species within the depth of a few micrometers was checked. (4) With a Raman microprobe spectrometer (JASCO NR1800) spectra of lattice vibrations in the surface region were measured and the crystallinity and the magnitude of strain in the sample was checked. The wavelength and the power of the incident light were 514.5 nm and 9 mW, respectively. The energy resolution of the spectrometer was 2.2 cm^{-1}.

III. RESULTS AND DISCUSSION

A. SH images of steps and holes on cleaved GaAs(110) surfaces

We have made various steps and holes on GaAs(110) surfaces by cleaving wafer substrates intentionally in a rough way. A typical microphotograph of a cleaved surface is shown in Fig. 2(a). Dark spots, e.g., the one labeled *A*, indicate holes, and dark lines indicate macroscopic steps about a few micrometers in height. Figure 2(b) shows a SH intensity image of the same sample, obtained with accumulation time of 1000 s. The SH intensity is strong where the image is bright. The excitation laser light illuminated the area in the white circle in Fig. 2(b). The polarizations of incident and observed light fields were parallel to each other, and the sample rotation angle ϕ was 50°. In this polarization configuration bulk SHG of GaAs is allowed. The integrated intensity of the SH intensity image as a function of the sample rotation angle ϕ agreed with the selection rule of SHG from bulk GaAs.

Let us first check how the steps and holes are seen in the SH intensity image in Fig. 2(b). Steps are seen as dark lines in the SH intensity image. Holes are also seen as dark spots in the SH intensity image, but they are hard to identify in Fig. 2(b). The reason why the SH intensity of steps and holes are weak is as follows. The SH light from terraces of the sample surface travels in the same direction as the reflected fundamental light and is captured by the objective lens. On the other hand, SH light from steps and holes travels in other directions and fails to enter the objective lens. Hence, steps and holes show weak SH intensity.

Let us next turn to the bright spots and patches labeled *B* and *C* in Fig. 2(b). In a microphotograph of Fig. 2(a), a slightly dark structure is seen at the position labeled *B*. On the other hand, we see no prominent structure but flat terraces in Fig. 2(a) at the position labeled *C*. Such bright spots and patches in the SH intensity images were frequently found. As will be discussed in detail in Sec. III B, this intense SHG is caused by an enhancement of the internal light field due to an optical interference in a slab structure. For this purpose we have selected a cleaved surface with a large area of intense second harmonic emission, and have analyzed it using the combination of various techniques.

B. SH intensity image of a slab structure

Figures 3(a) and 3(b) are a microphotograph and a SH intensity image of a cleaved surface of GaAs(110) with a

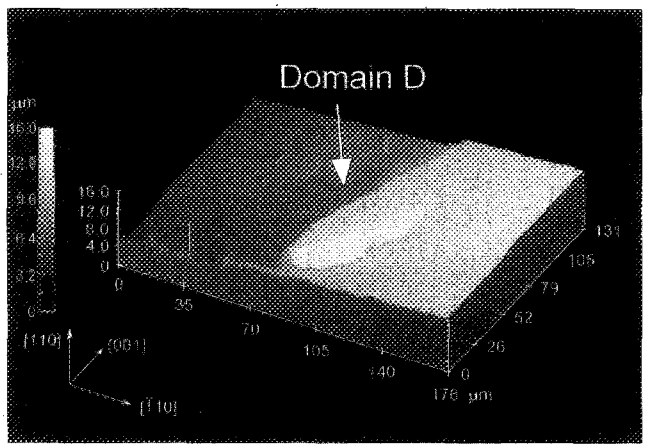

FIG. 4. Topograph of a cleaved GaAs surface near domain *D* observed with a confocal laser microscope.

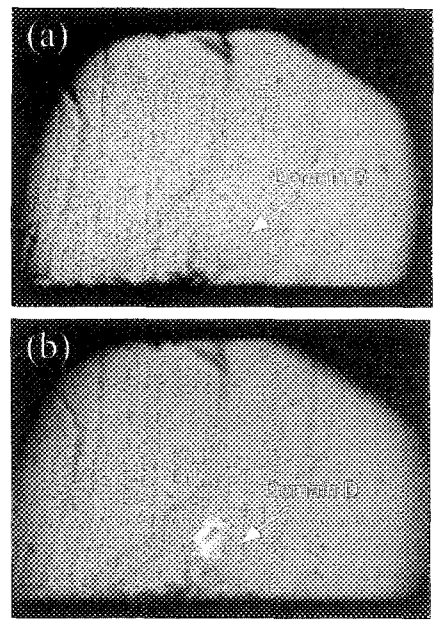

FIG. 5. Infrared reflected images of cleaved GaAs(110) near domain *D* with incident wavelengths: (a) 800 nm and (b) 880 nm.

relatively large area emitting intense second harmonic radiation, respectively. The SH image in Fig. 3(b) was taken with the accumulation time of 300 s. The incident and output polarizations were perpendicular to each other, and the sample rotation angle ϕ was 90°. This polarization configuration allows bulk SHG of GaAs. In Fig. 3(b) we see that SH intensity is enhanced in a considerably large domain. Let us call this domain domain *D*. Figure 3(c) shows the 1D SH intensity distribution in the region between the two parallel lines in Fig. 3(b). The SH intensity profile in Fig. 3(c) has four periodic peaks. The enhancement of the SH intensity in domain *D* relative to that outside domain *D* is estimated to be 20–100. In Fig. 3(a) domain *D* looks like a flat terrace. There is no remarkable difference in brightness between the terrace in domain *D* and the other terraces in Fig. 3(a).

Figure 4 shows a topograph of the same GaAs(110) surface, obtained with a scanning confocal laser microscope. Domain *D* is seen as a structure like an upheaved plate with the size of 30×80 μm^2 in Fig. 4. In order to confirm that there is no change of properties of the material itself in domain *D*, we have carried out electron probe microanalysis (EPMA) and Raman measurements. The result of the EPMA measurement showed that there are no differences in the chemical composition between domain *D* and the other domains. We have measured the intensity of TO phonon lines in domain *D* with a Raman microscope. The vibrational frequency, bandwidth, intensity, and polarization selection rule of the TO phonon in domain *D* are the same as those of pure GaAs.

Figures 5(a) and 5(b) are the infrared reflected images of the same sample at wavelengths of 800 and 880 nm, respectively. Domain *D* looks bright in Fig. 5(b), while it does not in Fig. 5(a). This difference in infrared reflectivity in domain *D* is interpreted as follows. The penetration depths of light of wavelength 800 and 880 nm are ~1 and ~15 μm in GaAs at room temperature, respectively. If there is a boundary such as an air gap in domain *D* at a depth deeper than 1 μm and shallower than 15 μm, the infrared light of wavelength at 880 nm will be reflected back by the boundary while that of wavelength at 800 nm will not. In this case domain *D* looks bright at 880 nm but not at 800 nm. Thus there should be such a boundary under the surface in domain *D*. This boundary or air gap will have been created by the cleavage of the sample. In addition, we have found that the brightness of domain *D* in Fig. 5(b) oscillates as a function of the incident wavelength near 880 nm due to optical interference. Thus we conclude that a slab structure is formed in the region of domain *D*. From the step height seen in Fig. 4, we assume that the thickness of the slab is estimated to be a few micrometers. This is consistent with the depth of the boundary suggested in the above discussion.

Now we will see whether the enhancement of SHG observed in Fig. 3(b) is caused by the slab structure in domain *D*. We have carried out a theoretical calculation of SH intensity based on the phenomenological SHG theory reported by Sipe *et al.*[12] Our calculation consists of three steps: (1) calculation of the electric field $E_m(\omega)$ in a slab structure under the incidence of light with the frequency of ω; (2) calculation of nonlinear polarization $P^{NL}(2\omega)=\chi^{(2)}:E_m(\omega)\,E_m(\omega)$ with a nonlinear susceptibility $\chi^{(2)}$; and (3) calculation of the radiated light intensity from the nonlinear polarization in the specular direction.

In the present calculation we have neglected the substrate material below the slab, because the contribution of the substrate material to the SHG signal can be roughly estimated to be less than one quarter of that of the slab. Then, to simplify the electromagnetic calculation, we considered a three-layered dielectric system consisting of vacuum, GaAs, and vacuum layers, as shown in Fig. 6. We considered only the bulk nonlinear response of GaAs and have neglected the surface nonlinear response as a contribution to SHG. The parameters used in the calculation were the wavelength of incident light $\lambda_{in}=1064$ nm, the incident angle $\theta=0°$, and the dielectric constants of GaAs $\epsilon(1064\,\text{nm})=12.1$ and $\epsilon(532\,\text{nm})=17.4+2.7i$.[13]

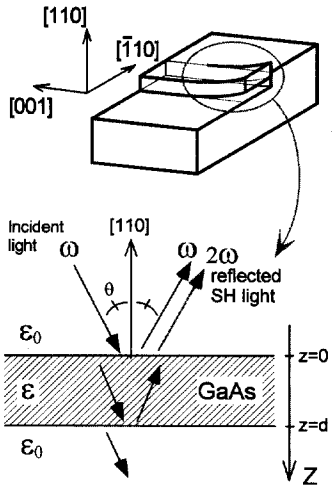

FIG. 6. Three-layered structure for a model calculation of reflected SH intensity from a slab on a cleaved GaAs surface. ϵ_0 and ϵ are the dielectric constants of vacuum and GaAs bulk, respectively. d is the thickness of the slab layer.

Figure 7 shows the calculated SH intensity from a GaAs slab as a function of the thickness d. The intensity is normalized to the calculated SH intensity in the case of infinite slab thickness. Namely, the vertical axis is the enhancement factor of the SH intensity from the slab structure relative to that from a two-layered system consisting of vacuum and GaAs layers. The enhancement factor periodically oscillates from 4 to 70 as a function of the thickness.

We can find the origin of this periodic enhancement of SHG by analyzing the calculated result. There are two fundamental electric fields propagating upward and downward in a GaAs slab. Because the reflectivity of the slab oscillates as a function of the thickness due to optical interference, the intensity of the upward- and downward-propagating internal electric field in a slab also oscillates periodically. The field propagating upward generates reflected SH radiation much more efficiently than the downward-propagating field. Hence the reflected SH radiation is enhanced periodically as a function of the slab thickness due to the periodic enhancement of the upward-propagating internal electric field. The SH intensity from a thick GaAs wafer is weaker than that from the present slab, because the SH light in this case is generated only by the downward-propagating field. If we consider the substrate layer below the slab in the SHG calculation, more complicated optical interference occurs in a four-layered dielectric system. In this case, however, the same mechanism of SHG enhancement as mentioned above can be expected.

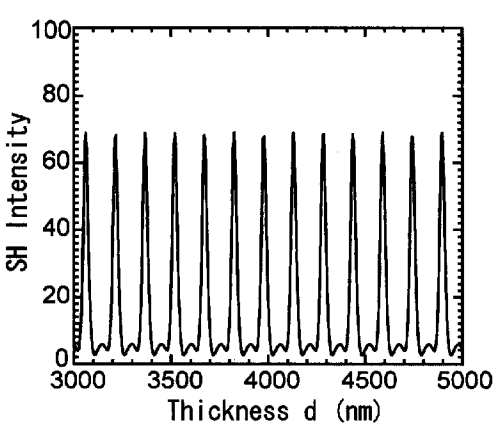

FIG. 7. Calculated SH intensity of a GaAs slab as a function of the thickness of the slab. The intensity is normalized to the calculated SH intensity in the case of infinite slab thickness.

The calculated results above well explain the features of the experimental result in Fig. 3(c), if we assume that the structure in the problem is a wedge slab or that the thickness of the slab varies as a function of position. Namely, we assume that the thickness of the slab varies if we move along the white lines in Fig. 3(b) on the slab. Thus the variation of the SH intensity as a function of position on the slab in Fig. 3(c) corresponds to that as a function of the slab thickness d in Fig. 7. The observed enhancement factor of 20–100 in Fig. 3(c) agrees well with the calculated enhancement factor of 4–70 in Fig. 7. This agreement indicates that the three-layered system used in our calculation is reasonable. From Fig. 3(c) the variation of the slab thickness is estimated to be about 600 nm from one end to the other of the slab.

With the results obtained above on domain D, we go back to Fig. 2(b) and consider the origin of the bright spots again. Following the above analysis on domain D, we have also observed infrared reflected images of this sample at a wavelength of 800–900 nm. Domain C in Fig. 2(b) showed oscillation of infrared reflectivity as a function of the observed wavelength. Hence this domain has a slab structure. Domain B in Fig. 2(b) did not show high infrared reflectivity. This is either because domain B is too small for infrared detection or because there is a GaAs dust particle created during the cleavage. Usually when GaAs dust particles are not removed after cleavage, we see many bright spots on the cleaved surface by a SH microscope, while we do not see corresponding structures in the infrared reflection image. These bright spots in SH intensity image disappear when we remove the dust particles.

The results obtained in this study strongly suggest that the SH microscope will be a powerful tool in the analysis of small structures on semiconductor surfaces. The image of slab structures obtained with a SH microscope has high contrast to the background, so we can identify them sensitively. We consider that this slab structure is a model case of buried structures in semiconductor devices. We will be able to pick up information on buried structures in semiconductor devices because semiconductors have high optical transmission at the excitation wavelength of SHG in the infrared region.

In addition to the observation of small structures on semiconductors, the application of the SH microscopy to surface analysis will be a fruitful development. The SHG method has monolayer sensitivity[14,15] and is capable of detecting surface electronic states.[3,4] Hence we will be able to observe spatial patterns of orientations or electronic states of surface adsorbates. These spatial patterns will give information on the driving forces of various surface phenomena such as crystal growth, catalytic reaction, and chemical reaction on electrodes.

IV. CONCLUSION

We have developed a highly sensitive SH microscope as a new surface probe and have observed small structures on a cleaved GaAs(110) surface. We also used a near infrared microscope, a confocal laser microscope, a Raman microprobe spectrometer, and an EPMA, to identify the observed structures. The SH intensity image of slab structures and GaAs dust particles has high contrast to the background, and gives a sensitive identification of these structures. The enhancement factor of the SH intensity by a slab structure can be well explained by electromagnetic calculation.

ACKNOWLEDGMENTS

The authors are grateful to H. Kita, E. Nakamura, and M. Uno of our Institute for their technical support. This work was supported in part by a Grant-in-Aid for Science Research from the Ministry of Education, Science, Sports, and Culture.

[1] H. H. Rotermund, Surf. Sci. **283**, 87 (1993).
[2] R. W. J. Hollering, J. Opt. Soc. Am. B **8**, 374 (1991).
[3] T. F. Heinz, F. J. Himpsel, E. Palange, and E. Burstein, Phys. Rev. Lett. **63**, 644 (1989).
[4] H. Tanaka, G. Mizutani, and S. Ushioda, Surf. Sci. **402–404**, 533 (1998).
[5] H. Tanaka, H. Kurokawa, E. Kobayashi, H. Sano, G. Mizutani, and S. Ushioda, Prog. Cryst. Growth Charact. Mater. **33**, 129 (1996).
[6] D. Ding, T. Käämbre, S. Ljungström, Y. Chen, K. Siegbahn, E. Wistus, P. Swensson, and E. Mukhtar, Appl. Surf. Sci. **96–98**, 581 (1996).
[7] M. Fiebig, Fröhlich, G. Sluyterman v. L. , and R. V. Pisarev, Appl. Phys. Lett. **66**, 2906 (1995).
[8] S. Kurimura and Y. Uesu, J. Appl. Phys. **81**, 369 (1997).
[9] I. I. Suni and E. G. Seebauer, J. Chem. Phys. **100**, 6772 (1994).
[10] Y. Sonoda, G. Mizutani, H. Sano, S. Ushioda, T. Sekiya, and S. Kurita, Jpn. J. Appl. Phys. (submitted).
[11] C. Yamada and T. Kimura, Phys. Rev. B **49**, 14372 (1994).
[12] J. E. Sipe, D. J. Moss, and H. M. van Driel, Phys. Rev. B **35**, 1129 (1987).
[13] R. K. Williardson and A. C. Beer, *Semiconductors and Semimetals*, Optical Properties of III-V Compounds, Vol. 3 (Academic, New York, 1967).
[14] W. Chen, M. B. Feller, and Y. R. Shen, Phys. Rev. Lett. **63**, 2665 (1989).
[15] T. Yamauchi, Y. Sonoda, K. Sakamoto, S. Ushioda, H. Sano, J. Sakai, and G. Mizutani, Surf. Sci. **363**, 385 (1996).